

See discussions, stats, and author profiles for this publication at: <https://www.researchgate.net/publication/267330574>

Correlation between Optical Properties and Nanomorphology of Fluoranthene-Based Conjugated Copolymer

ARTICLE *in* THE JOURNAL OF PHYSICAL CHEMISTRY C · JULY 2014

Impact Factor: 4.77 · DOI: 10.1021/jp5040079

CITATION

1

READS

36

3 AUTHORS, INCLUDING:



Joydeep Dhar

Jadavpur University

8 PUBLICATIONS 58 CITATIONS

[SEE PROFILE](#)



Shiv Kumar

Indian Institute of Science

7 PUBLICATIONS 135 CITATIONS

[SEE PROFILE](#)

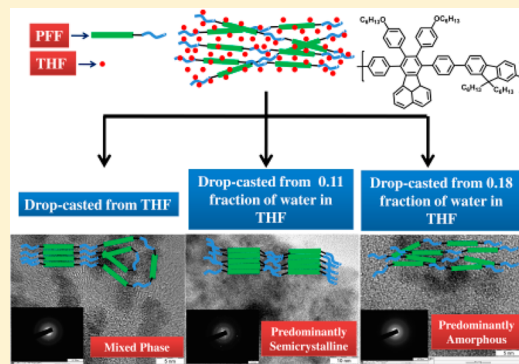
Correlation between Optical Properties and Nanomorphology of Fluoranthene-Based Conjugated Copolymer

Joydeep Dhar,[†] Shiv Kumar,[†] and Satish Patil*

Solid State and Structural Chemistry Unit, Indian Institute of Science, Bangalore 560012, India

S Supporting Information

ABSTRACT: Nanoparticles of conjugated polymers are receiving attention due to their interesting optical properties. Here we report nanoparticles of fluoranthene-based conjugated copolymer prepared by the Suzuki coupling reaction. The copolymer forms nanoparticles by the spontaneous self-assembly after evaporation of organic solvent. The mean diameter of the nanoparticles can be manipulated by varying solvent composition. We investigated the parameters that govern the nanostructured morphology of polymer by systematic variation of good and poor solvent. The UV-vis and time-resolved fluorescence spectroscopy measurement reveal the use of poor solvent in the organization of nanostructures. Furthermore, transmission electron microscopy highlights the importance of rigidity of the polymer backbone in morphological development.



1. INTRODUCTION

π -Conjugated polymeric nanoparticles (CPNs) have found a wide range of applications as active materials in fluorescence imaging,¹ nanomedicine,² optoelectronic devices,³ and sensors.⁴ The emergence of CPNs as materials of research interest is due to their unique physicochemical properties as compared to the bulk polymers.⁵ A myriad of methods for fabrication of CPNs are reported in the literature. Among various methods, miniemulsion is the most favored and extensively adopted owing to their apparent advantages such as very small particle size accompanied by a narrow size distribution.^{6–8} However, the method involves use of stabilizer, which in turn limits their practical applications.⁹ Hence, alternative facile methods such as reprecipitation have been explored for preparation of CPNs.^{10–12} In this method, triggering the collapse of polymer chain from the solvated environment in a good solvent by adding a poor solvent leads to the formation of well-dispersed nano- or micron-sized particles.¹³ Vivid characterization of these particles to gain insight about structure and in turn their property is a preliminary requisite to explore their utilities as a functional material. In recent years, this procedure has attracted widespread of interest as a synthetic protocol for preparation of nanoparticles from conjugated polymers, but there is still dearth of decipherable understanding about the underlying mechanism of formation and growth of the nanoparticles in the literature.¹⁴ In this paper, we have investigated the correlation of optical properties of the nanostructure varied in structural and morphological features from the newly synthesized copolymer based on two chromophores: fluoranthene and fluorene (viz. PFF). The present work deals with the synthesis of conjugated polymer and detailed studies of self-assembling in mixed solvents.

A number of research groups have reported the preparation of CPNs by incorporation of fluorene in polymer backbone and demonstrated that fluorene moiety assists to form spherical nanoparticle from different block copolymer.^{8,12,15,16} On the other hand, phenyl-substituted fluoranthene unit provides rigidity and crystallinity in the molecular structure.^{17,18} The charge carrier mobility in polymeric semiconductors depends on the π -orbital overlap along the conjugated backbone which improves with the planarity and rigidity of the repeating unit. In this respect, fluoranthene-based polymer has gained tremendous interest as it provides planarity to the molecular architecture with extended π -conjugation.¹⁸ The most promising properties of fluoranthene derivatives for organic light-emitting diodes (OLEDs) are its wide band gap, long lifetime, high quantum yield, apparent resistance to quenching/eximer emission, electrochemical stability, and easy functionalization.¹⁹ It is highly promising chromophore for potential use in OLEDs and organic photovoltaics (OPVs).^{20–22} Our design principle is based on these rationales where we combine these two chromophores (fluorene and fluoranthene) to synthesize the copolymer with novel properties. Copolymer with alternate conjugation of these two monomers has provided a fine balance between rigidity and flexibility in molecular architecture rendering the scope to manipulate its self-assembling behavior by varying the solvent composition. It is well documented that the chain conformations of rigid π -conjugated polymer is driven by surrounding environment and the range of conformations were observed based on the polarity of solvents.²³ In our

Received: April 24, 2014

Revised: June 19, 2014

Published: July 1, 2014



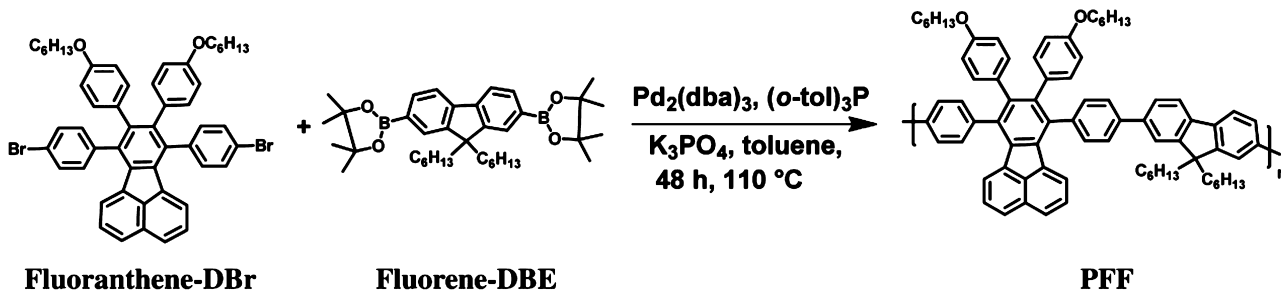
ACS Publications

© 2014 American Chemical Society

15079

dx.doi.org/10.1021/jp5040079 | J. Phys. Chem. C 2014, 118, 15079–15085

Scheme 1. Synthesis of PFF by Suzuki Cross-Coupling Reaction



present study, we have observed that solvent polarity imparts drastic alteration of optical properties of fluoranthene-based conjugated copolymer. We have investigated distinct features observed under microscopic studies which promote the designated changes in optical properties of the copolymer. We realize from our experimental findings that the change in nanomorphology was one of the governing factors to have a direct correlation in structure-dependent optical properties.

2. MATERIALS AND METHODS

2.1. Materials. Tri(*o*-tolyl)phosphine ($(\text{o-tol})_3\text{P}$) and tris(dibenzylideneacetone)dipalladium(0) ($\text{Pd}_2(\text{dba})_3$) were purchased from Sigma-Aldrich. Potassium phosphate (K_3PO_4), toluene, chloroform, dichloromethane, tetrahydrofuran (THF), hydrochloric acid, and methanol were supplied by SD Fine Chemicals. The chemicals were used without further purification. Polyfluorene (PF6) was synthesized by Suzuki coupling reaction as reported in the literature.²⁴

2.2. Methods. UV-Vis Spectroscopy. Absorption spectra of monomers and polymer in THF and thin film were recorded on a PerkinElmer (Lambda 35) spectrometer. All the experiments were carried out at room temperature.

Fluorescence Spectroscopy. Steady state fluorescence spectra were collected on a Horiba JovinYvon Fluorolog4 fluorometer, and quantum yield was determined using an integrated sphere. The steady state emission spectra were recorded by exciting the polymer at 339 nm in THF. Time-dependent fluorescence measurements were performed in solution with a Horiba JovinYvon lifetime spectrometer (TCSPC) with laser diode (369 nm, 25 ps) and emission monitored at 470 nm.

Gel Permeation Chromatography (GPC). Average molecular weights (M_w , M_n) were determined by gel permeation chromatography (GPC) against polystyrene standards using the Waters GPC system. THF was used as eluent with a flow rate of 1 mL/min.

Field-Emission Scanning Electron Microscopy (FESEM). Samples were prepared by drop-casting the nanoparticle dispersion on silicon wafer. FESEM imaging was performed using a Zeiss scanning electron microscope at 5 kV after gold coating.

Dynamic Light Scattering (DLS). Particle size was determined in solutions using ZetaPALS potential analyzer, Brookhaven Instruments Corp., Holtsville, NY.

Transmission Electron Microscopy (TEM). TEM images were taken in Zeol field emission microscope at 200 kV at room temperature. A dilute solution of nanoparticle dispersion was drop-casted on carbon-coated copper grid and dried in air.

Atomic Force Microscopy (AFM). AFM images were obtained by using the Bruker AFM instrument in tapping

mode by drop-casting nanoparticle dispersion onto a silicon wafer.

Electrochemical Studies. Redox property of the copolymer PFF was evaluated by cyclic voltammetry experiment (CH instrument). Ag/AgCl was used as a reference electrode whereas Pt was employed as both working and counter electrodes. Dry acetonitrile and tetrabutylammonium hexafluorophosphate (0.1 mol/L) were used as solvent and supporting electrolyte, respectively. Ferrocene/ferrocenium redox couple was used as standard for calibration. At similar experimental condition the oxidation of ferrocene was observed at 0.3 V vs the Ag/AgCl electrode. The oxidation potential for ferrocene/ferrocenium couple corresponds to the absolute energy level of -4.8 eV with respect to the vacuum. Highest occupied molecular orbital (HOMO), lowest unoccupied molecular orbital (LUMO), and corresponding band gap were calculated from the oxidation and reduction potential. The positions of HOMO and LUMO were computed from the equation, and band gap was determined from the difference between them.

$$\text{HOMO} = -(E_{\text{ox}} + 4.5) \text{ eV}; \quad \text{LUMO} = -(E_{\text{red}} + 4.5) \text{ eV}$$

3. RESULTS AND DISCUSSION

Synthesis of PFF. The copolymer (PFF) was synthesized by Suzuki cross-coupling reaction of 7,10-bis(4-bromophenyl)-8,9-bis(4-hexyloxy)phenyl)fluoranthene (Fluoranthene-DBr) and 2,2'-(9,9-dihexyl-9H-fluorene-2,7-diyl)bis(4,4,5,5-tetramethyl-1,3,2-dioxoborolane) (Fluorene-DBE) using $\text{Pd}_2(\text{dba})_3$ and $(\text{o-tol})_3\text{P}$ as catalyst and ligand as shown in Scheme 1. The detailed synthesis procedure of the monomers and polymer are given in the Supporting Information. The copolymer was purified by precipitation in methanol/hydrochloric acid followed by Soxhlet extraction using methanol, hexane, and acetone to ensure complete removal of catalytic impurities and undesired low molecular weight oligomers, and finally reprecipitation in methanol gave a pale green solid. ^1H and ^{13}C NMR spectra of PFF are given in Figure SI 1 of the Supporting Information.

Number-averaged molecular weight (M_n) of 7477 g/mol and weight-averaged molecular weight (M_w) of 14 993 g/mol with a polydispersity of 2.0 were obtained from gel permeation chromatography (GPC) studies (Figure SI 2, Supporting Information). The copolymer shows the broad absorption spectrum in THF having two absorption maxima at 305 nm (A_{305}) and 340 nm (A_{340}); both the bands correspond to $\pi \rightarrow \pi^*$ transitions (Figure 1). Thin film absorption spectrum is similar to the solution state spectrum except minor changes in the peak ratio A_{340}/A_{305} which indicates that molecular arrangement and interactions are quite similar in solution and

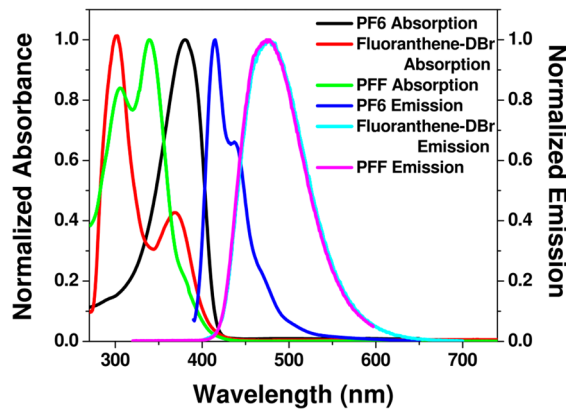


Figure 1. Absorption and emission spectra of the corresponding monomer and polymers in THF.

solid state (Figure SI 3, Supporting Information). The structured absorption characteristic of the copolymer was not observed in fluorescence spectra. PFF exhibits featureless broad emission with maxima at 476 nm in solution as well as in the solid state. Similar to the absorption spectra, no change is observed in the photoluminescence spectrum of thin film in comparison with the solution (Figure SI 3, Supporting Information). The emission spectrum is complete resemblance to the fluorescence of fluoranthene monomer (Fluoranthene-DBr) (Figure 1), implying the fluoranthene unit plays a dominant role in photoluminescence of the copolymer as emission from the poly(fluorene) (PF6) exhibits vibronic characteristic.²⁵ The optical band gap of PFF was found to be 3.02 eV. A cyclic voltammetry (CV) experiment was carried out to determine the position of the frontier molecular orbitals of the copolymer. The voltammograms are given in Figure SI 4 of the Supporting Information. The energy values of HOMO and LUMO were calculated as -5.90 and -3.02 eV, respectively.

Ground state geometry of a single repeating unit of the polymer was optimized and electron density distribution in the frontier molecular orbitals were elucidated by density functional theory (DFT) calculations employing B3LYP hybrid functional with 6-31g* basis set. The hexyl and hexyloxy groups were replaced with methyl and methoxy chains to reduce the computational time. The ground state optimized geometry exhibits nonplanarity of the molecular backbone. Phenyl rings attached to the fluoranthene core stay out of the plane, almost vertically to minimize the steric hindrance. The wave functions are localized over the fluoranthene in the frontier molecular orbitals, e.g. HOMO and LUMO, respectively (Figure 2). We have not observed delocalization of electron density on fluorene moiety. Time-dependent DFT (TD-DFT) calculations were carried out to determine the orbitals associated with the electronic transition, and the results are summarized in Table 1. We have observed that three transitions are associated with the absorption band extending from 300 to 400 nm. Out of three transitions, the HOMO-1 → LUMO calculated to be the strongest one. The orbitals related to those transitions do not have the electron density on the fluorene moiety; therefore, we do not notice any effect of fluorene unit in optical properties of the polymer. Hence, our theoretical calculations support the results observed in optical studies.

The unique feature of this copolymer lies in its inherent tendency to undergo concentration-independent, self-assembly in different organic solvents, such as chloroform and THF. We

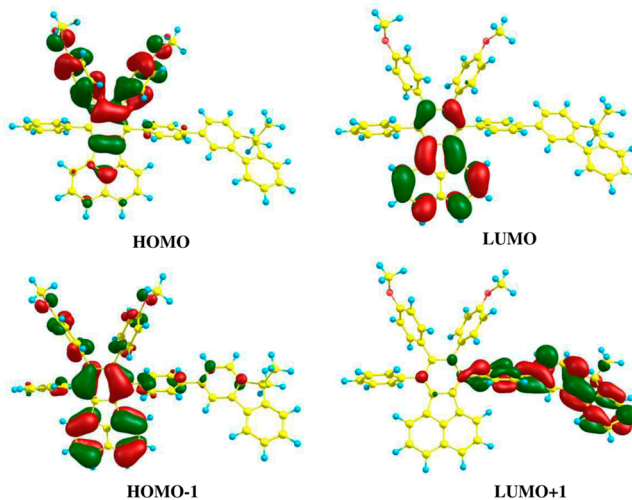


Figure 2. Optimized ground state geometry with electron distribution of frontier molecular orbital of the repeating unit of the polymer. Electron density distributes over fluorene moiety in LUMO+1 orbital, though this orbital does not participate in electronic transition.

observed the formation of inhomogeneous spherical or quasi-spherical assembly with interconnected network in the nanometer domain by drop-casting a film from THF. In the reprecipitation method, we obtained highly uniform spherical nanoparticles by fast addition of copolymer solution (dissolved in THF) into water under strong stirring conditions. We observed the instantaneous formation of nanoparticles with narrow size distribution. But, while following this procedure, we were unable to control the size or optical property of obtained nanostructured materials and in turn motivated us to pursue its reverse technique to finely tune the structure and property in a controlled fashion. We opted to add varying quantity of water, a poor solvent into the fixed concentration of the copolymer dissolved in THF. The polymer concentration was fixed at 0.25 mg/mL in THF, and a different volume of water was injected, starting from 5 to 45 μL with regular interval of 10 μL to prepare five sets of samples in 0.2 mL of THF solution. We have calculated the volume fraction of water for each of the samples, and all the data have been given in the water fraction throughout the article. The calculated volume fraction of water for respective sample is shown in Table 2. Addition of water enhances the polarity of the environment and polymers tend to aggregate.

Depending on the volume fraction of water, the degree of aggregation of the copolymer chain varies, resulting in particle size distribution and morphology of the nanoaggregates. This was clearly reflected in their optical spectra (Figure 3a) in the solid state. Thin film absorption spectra of the samples prepared with different volume fraction of water showed a blue-shift as compared to the sample in THF. The blue-shift may be due to decrease in conjugation as polymer adopt collapsed conformation,²⁶ but the extent of deviation varied depending on the nature of the samples. Significant blue-shifts of 50 and 85 nm were observed for the samples with 0.02 and 0.07 volume fraction of water, respectively. But there was an exception; surprisingly for the sample S4, prepared at 0.11 water fraction showed a red-shift as compared to the previous two samples. This clearly indicates that the polymer regains ordered structures and is believed to adopt stretched conformation. On the basis of these observations, we anticipate

Table 1. Summary of Excited State Electronic Transitions Obtained from TD-DFT Calculations

compd	dominant contribution	absorption (nm)	energy (eV)	oscillator strength (f)	dipole moment (D)
PFF	H-1 → L (67.99%)	365.88	3.38	0.2197	2.65
	H → L (67.95%)	394.79	3.14	0.0389	
	H-4 → L (52.39%)	347.17	3.57	0.0121	

Table 2. Sample Compositions Prepared in THF/Water

sample	THF (mL)	water (mL)	vol fraction of water
S1	0.2	0	0
S2	0.2	0.005	0.02
S3	0.2	0.015	0.07
S4	0.2	0.025	0.11
S5	0.2	0.035	0.15
S6	0.2	0.045	0.18

that the conjugation length increases in the sample S4. For remaining two samples, S5 and S6, with 0.15 and 0.18 volume fraction of water, a further blue-shift of more than 150 nm with well-defined maxima was observed. The long tail in the absorption spectra indicates the presence of different low-energy chain conformation due to the aggregation of the polymer chain. The solution state absorption spectra (Figure SI 5, Supporting Information) of the polymer samples S1–S6 exhibit minor change in optical properties. The peak ratio A_{340}/A_{305} , which is sensitive to the aggregation of polymer chains, alters with gradual increase in water content, but the shift was not as significant as what we have observed in solid state absorption spectra. Hence, we believe that aggregation is much more pronounced after evaporation of the solvent, although some preorganization in the solution cannot be discounted.

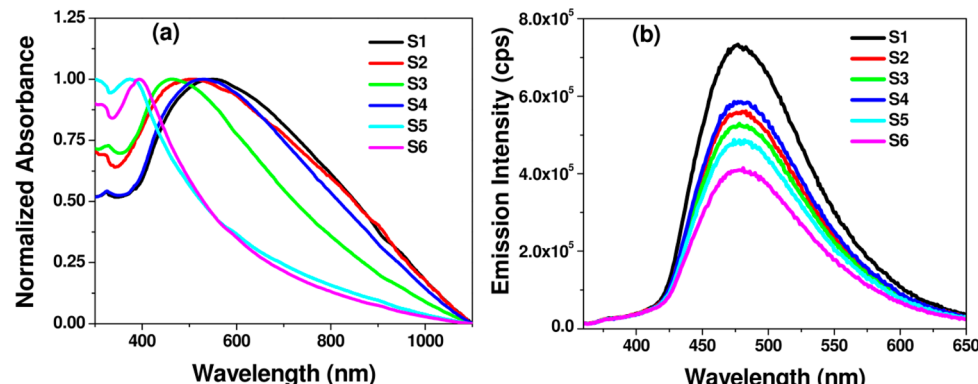
Copolymer solution in THF showed maximum intensity in fluorescence while emission gradually decreased with an increase in the amount of water due to enhancement in nonradiative decay pathway (Figure 3b). Similar to the UV-vis spectra, after adding 25 μ L, i.e. at 0.11 volume fraction of water emission intensity abruptly increases beyond the fluorescence observed for the samples prepared using varying amounts of water. This concentration marked a transition in morphology of nanoaggregates visualized from scanning/transmission electron microscopy (discussed later). A further increase in the water fraction reduced the intensity of the fluorescence, though the peak maxima for all the samples remained the same (476 nm).

The spectroscopic studies were further correlated with FESEM observations. Figure 4b–f shows the SEM images of samples prepared by the addition of different volume fraction of

water. As shown in Figure 4a, the copolymer self-assembles in a spherical manner and interconnected through fiber-like structure in the absence of water. At 0.02 volume fraction of water, the fiber-type structures merged together to form nanoparticles without well-defined surface boundary. Besides, the morphology of the particles is quite distinct from those prepared by drop-casting the polymer solution from THF. Well-separated bigger particles having diameter of ~300–500 nm with higher polydispersity in size were formed for sample S3, and thus we notice that a gradual increase in volume fraction of water assists to attain well-defined shape and size for the copolymer nanoparticles. When we reach the critical water fraction, i.e. 0.11 where already a transition in absorption and fluorescence emission was observed, we found that almost all the nanostructures have collapsed and very few particles were present with their structural integrity. Subsequently, increase in volume fraction of water (S5) again assisted the polymer chain to self-assemble in a spherical manner. The nanoparticles prepared at 45 μ L of water content showed the least polydispersity and small particle size among all other samples having diameter of ~150–200 nm with highest blue-shift in the absorption spectra.

The dynamic light scattering (DLS) study also indicates the presence of self-assembled nanostructure in solution. However, the average size measured from DLS (Figure SI 6, Supporting Information) was distinct from what we have observed in SEM images. This indicates that the nanoparticles were not well separated but remained clustered. The transmission electron microscopic (TEM) (Figure 6) and atomic force microscopy (AFM) (Figure SI 7, Supporting Information) images further corroborated our findings.

We have performed time-dependent fluorescence study to determine the lifetime of excited state species with gradual addition of water (Figure 5a). We observe that the lifetime of polymer show morphology-dependent behavior. Pristine polymer dissolved in THF showed biexponential decay profile with a lifetime of 0.5 and ~12 ns with a corresponding amplitudes of ~1% and ~99%, respectively. For PF6 and Fluoranthene-DBr, the observed fluorescence lifetimes were

**Figure 3.** Solid state absorption (a) and solution state emission (b) spectra of the self-assembled polymeric nanostructure.

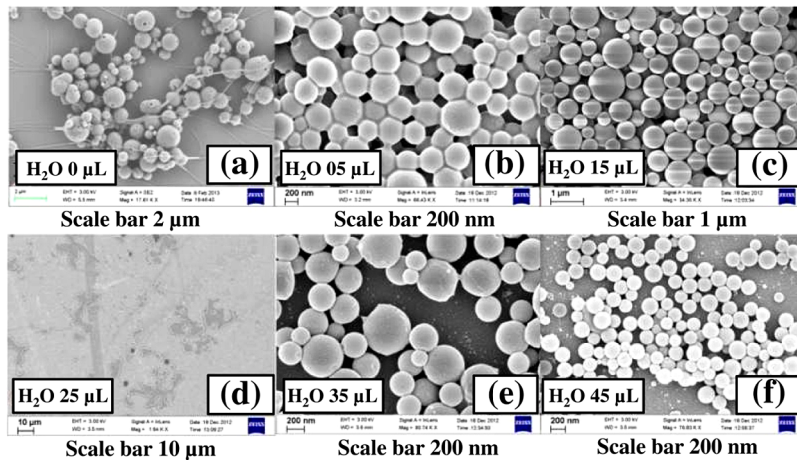


Figure 4. FESEM images of the self-assembled nanostructures in the presence of different volume fractions of water.

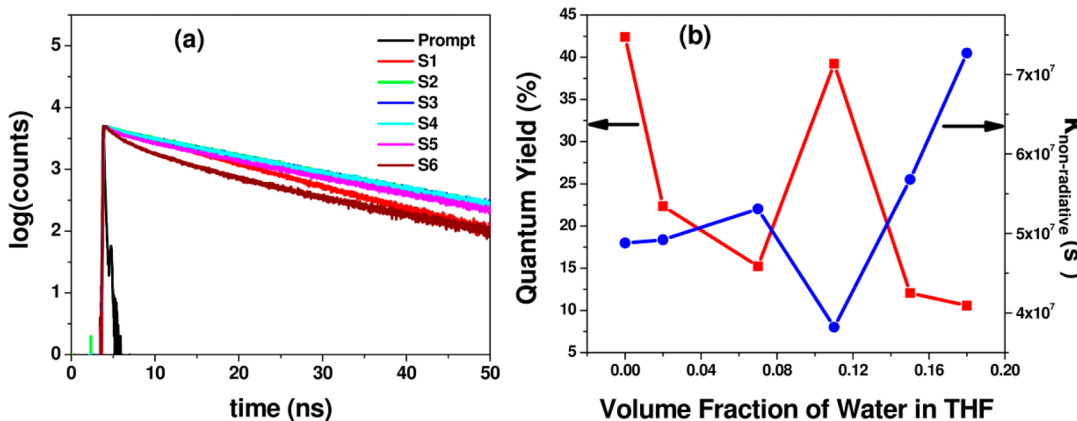


Figure 5. Fluorescence excited state decay profile (a) and quantum yield and corresponding nonradiative rate constants ($k_{\text{nonradiative}}$) of PFF in different water fractions (b).

0.56 and 8.6 ns, respectively.^{17,27} We have assigned the shortest and longest lifetime species from PFF to the fluorene and fluoranthene moieties. The photoluminescence and TD-DFT data suggest that the electronic transition from fluoranthene moiety dominates over fluorene component. As a result, the amplitude related to the short-lived species is almost inconsequential. The lifetime and corresponding amplitude of the major excited state constituent from different nanoparticle dispersions as well as of native polymer in THF have been summarized in Table 3. A complete description of all the excited species is provided in the Supporting Information (Table T1).

Table 3. Fluorescence Lifetime with Corresponding Amplitude of Major Excited State Species and Quantum Yield of PFF Prepared in Different Volume Fraction of Water

sample	amplitude (%)	τ (ns)	quantum yield (%)
S1	98.82	11.94	42.41
S2	98.99	15.94	22.31
S3	98.83	16.14	15.22
S4	98.70	16.11	39.23
S5	96.38	16.00	12.06
S6	71.88	15.61	10.57

As water fraction was gradually increased, the lifetime related to fluoranthene and fluorene increased proportionately. Upon addition up to 0.11 volume fraction of water the amplitudes of both the excited state species remained almost the same, but there was a commensurate enhancement in fluorescence lifetime. Higher water fraction (0.15) has changed the ratio of short to long-lived species with sharp enhancement of the lifetime of the shorter one resulting faster decay in S5 as compared to previous samples. A further increase in the water content (S6) breaks down the biexponential regime to triexponential decay pattern and generates a new excited state species with intermediate lifetime and amplitude of 4.6 ns and $\sim 25\%$ (Table T1, Supporting Information). Variation in fluorescence quantum yield qualitatively agrees with the steady state fluorescence emission spectra as shown in Figure 5b. PFF in THF showed a higher quantum yield of 42% which gradually diminished with the addition of water. Only the sample S4 demonstrated its unusual behavior with steep rise in quantum yield (39%) complied by a drop in quantum yield with higher fraction of water. We attribute size-dependent variation in quantum yield to the energy transfer between intrachain aggregates acting as quenching sites present in the nanoparticles.²⁸ To assign such energy transfers or quenching sites for exciton, we have calculated $k_{\text{radiative}}$ and $k_{\text{nonradiative}}$ (rate constants). The radiative ($k_{\text{radiative}}$) and nonradiative rate-constants ($k_{\text{nonradiative}}$) of PFF in various solvent compositions are summarized in Table T2 of the Supporting Information.

Other than S6, the average excited state lifetime gradually increases from S1 to S5. As a result, we see a parallel decrease in $k_{\text{radiative}}$ leading to the decrease in quantum yield except for the sample S4.

The $k_{\text{nonradiative}}$ for all the samples gradually increases by adding water in THF, but at the transition point (S4) the nonradiative decay pathway was retarded, and we observe enhancement in quantum yield. The $k_{\text{nonradiative}}$ for S6 sample was too high to observe any significant increase in quantum yield, though the $k_{\text{radiative}}$ has increased as compared to the previous sample, S5. Hence, the sample S4 exhibited a high quantum yield due to the stabilization of excited state by suppressing the nonradiative energy loss mechanism.

The mechanism of formation of nanoparticles is believed to be due to the collapse in polymer chain conformations leading to the formation of these particles. As we have observed, gradual morphological changes with the addition of water suggest that polymer prefers to have a spherical morphology despite the rigidity of the polymer chains. Poly(fluorene) has a natural propensity to constitute a well-defined structure as it has been observed in different studies.^{1,29} On the contrary, the π -conjugated planar molecule such as fluoranthene prefers to stack in 1D or 2D orientation due to their rigidity and crystallinity.¹⁸ These parameters control the growth and dimensionality of the self-assembly of π -conjugated polymers. Incorporating two monomeric units of such a type in an alternate fashion in PFF, the size and morphology of the nanoparticles were controlled by balancing these two opposing forces, as mentioned earlier. Our apprehension about the structural variation was well supported by transmission electron microscopy. The nanoscale organization during self-assembly was evidenced with high-resolution TEM (HRTEM) and selected area electron diffraction (SAED) pattern. The nanostructured of PFF were composed of both crystalline and amorphous phases which are a common characteristic observed for conjugated polymers. We found significant variation in packing imparted with gradual addition of water. Figure 6a shows the TEM image of the nanostructure prepared from THF. The particles appeared in quasi-spherical shape with quite broad size distribution (Figure 6a).

In HRTEM (Figure SI 8a, Supporting Information), few small crystalline domains with the predominant amorphous region were observed, and it was well supported by the SAED pattern (Figure 6b). The weak and diffusive diffraction rings in the SAED pattern (measured d -spacings were 3.6, 5.5, and 6.3 Å) indicate the copolymer chain adopts the mixed ordered/disordered arrangement, and the ordered arrangement is limited to the few repeating units of the polymer chain. But crystallinity gradually enhanced with the addition of water, and maximum crystallinity was observed in HRTEM and corresponding SAED pattern for PFF nanostructure at the critical point where collapsed morphology was observed (Figure 6c). At 0.11 volume fraction of water the nanostructure appears semicrystalline with variable d -spacing, implying polymer chains were highly orienting but the packing was random. Different d -spacings were calculated for this sample ranging from 2.3 to 8 Å. The inconsistent and multiple bright diffraction spots in the SAED pattern (Figure 6d) are complementary of HRTEM image (Figure SI 8b, Supporting Information), suggesting a polymer chain collapsed too rapidly to have any long-range order. On the other side, a higher fraction of water, e.g. 0.18, produces smaller, homogeneously distributed spherical nanoparticles having least crystallinity as

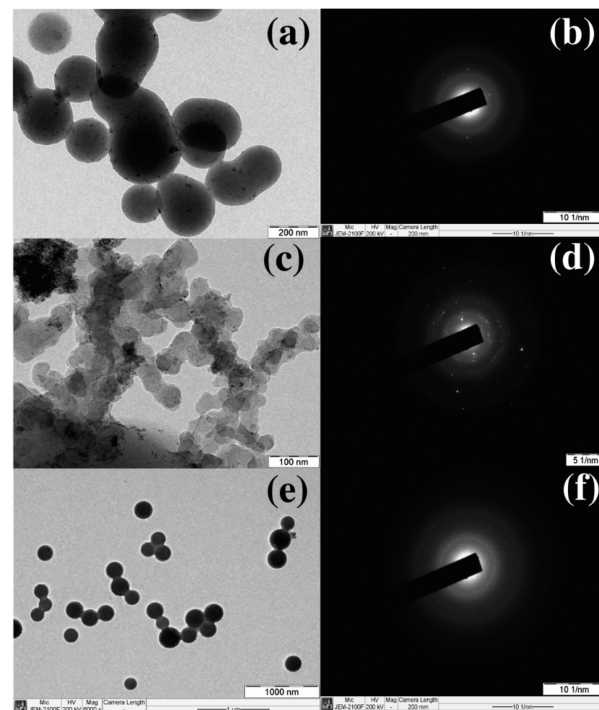


Figure 6. Representative bright field TEM images (a, c, e) and SAED pattern (b, d, f) of the samples prepared from S1 (a, b), S4 (c, d), and S6 (e, f).

shown in Figure 6e. Though the nanoparticles prepared at this water concentration were spherical in shape with very narrow size distribution, the particle morphology turned almost to be amorphous with extremely small crystallites (Figure SI 8c, Supporting Information). The SAED pattern was completely devoid of any diffraction spot (Figure 6f). Variation in crystallinity observed in the diffraction pattern in TEM supports the transition observed in optical measurement which corroborates our assumption.

4. CONCLUSION

In conclusion, nanoparticles of copolymer based on fluorene and fluoranthene were prepared by the reverse reprecipitation method. The optical properties of nanoparticles were studied by absorption and fluorescence spectroscopy. The results obtained from spectroscopy reveal a strong correlation of morphology of nanoparticles and critical role of poor solvent. Furthermore, the size and shape of nanostructures were tuned by the addition of a poor solvent, and the subsequent change in nanomorphology is attributed to different possible chain conformations of polymer. The photophysical and microscopic studies correlate well to elucidate the influence of rigidity of the polymer backbone rendered by fluoranthene moiety in evolution of nanomorphology. Transition to a complete amorphous coil-like conformations by adding water from a semirigid coil conformation in THF through a planar and crystalline phase is a quite unique observation in polymer self-assembly. We believe that rational design of semirigid polymer backbone with the inclusion of fluoranthene provides the necessary and delicate balance to have structural flexibility in visualizing such morphological evolution. This work highlights the unusual aggregation phenomenon of fluoranthene based π -conjugated polymers in a mixture of solvents.

■ ASSOCIATED CONTENT

Supporting Information

Experimental details, additional spectra, cyclic voltammogram, DLS, AFM, HRTEM, XRD images, detailed excited state lifetime, and radiative and nonradiative rate constants. This material is available free of charge via the Internet at <http://pubs.acs.org>.

■ AUTHOR INFORMATION

Corresponding Author

*E-mail: satish@sscu.iisc.ernet.in (S.P.).

Author Contributions

[†]These authors contributed equally.

Notes

The authors declare no competing financial interest.

■ ACKNOWLEDGMENTS

The authors acknowledge the Department of Science and Technology, New Delhi, India, for financial support. Joydeep Dhar and Shiv Kumar acknowledge Council of Scientific and Industrial Research (CSIR) and University Grant Commission (UGC) for Senior Research Fellowship (SRF), respectively.

■ REFERENCES

- Wu, C.; Bull, B.; Szymanski, C.; Christensen, K.; McNeill, J. Multicolor conjugated polymer dots for biological fluorescence imaging. *ACS Nano* **2008**, *2*, 2415–2423.
- Fernando, L. P.; Kandel, P. K.; Yu, J. B.; McNeill, J.; Ackroyd, P. C.; Christensen, K. A. Mechanism of cellular uptake of highly fluorescent conjugated polymer nanoparticles. *Biomacromolecules* **2010**, *11*, 2675–2682.
- Piok, T.; Gamerith, S.; Gadermaier, C.; Plank, H.; Wenzl, F. P.; Patil, S.; Montenegro, R.; Kietzke, T.; Neher, D.; Scherf, U.; Landfester, K.; List, E. J. W. Organic light-emitting devices fabricated from semiconducting nanospheres. *Adv. Mater.* **2003**, *15*, 800–804.
- Feng, J. C.; Li, Y.; Yang, M. J. Conjugated polymer-grafted silica nanoparticles for the sensitive detection of TNT. *Sens. Actuators, B* **2010**, *145*, 438–443.
- Kurokawa, N.; Yoshikawa, H.; Hirota, N.; Hyodo, K.; Masuhara, H. Size-dependent spectroscopic properties and thermochromic behavior in poly(substituted thiophene) nanoparticles. *ChemPhysChem* **2004**, *5*, 1609–1615.
- Landfester, K.; Montenegro, R.; Scherf, U.; Guntner, R.; Asawapirom, U.; Patil, S.; Neher, D.; Kietzke, T. Semiconducting polymer nanospheres in aqueous dispersion prepared by a miniemulsion process. *Adv. Mater.* **2002**, *14*, 651–655.
- Baier, M. C.; Huber, J.; Mecking, S. Fluorescent conjugated polymer nanoparticles by polymerization in miniemulsion. *J. Am. Chem. Soc.* **2009**, *131*, 14267–14273.
- Negele, C.; Haase, J.; Leitenstorfer, A.; Mecking, S. Polyfluorene nanoparticles and quantum dot hybrids via miniemulsion polymerization. *ACS Macro Lett.* **2012**, *1*, 1343–1346.
- Tuncel, D.; Demir, H. V. Conjugated polymer nanoparticles. *Nanoscale* **2010**, *2*, 484–494.
- Wu, C. F.; McNeill, J. Swelling-controlled polymer phase and fluorescence properties of polyfluorene nanoparticles. *Langmuir* **2008**, *24*, 5855–5861.
- Szymanski, C.; Wu, C. F.; Hooper, J.; Salazar, M. A.; Perdomo, A.; Dukes, A.; McNeill, J. Single molecule nanoparticles of the conjugated polymer MEH-PPV, preparation and characterization by near-field scanning optical microscopy. *J. Phys. Chem. B* **2005**, *109*, 8543–8546.
- Adachi, T.; Tong, L.; Kuwabara, J.; Kanbara, T.; Saeki, A.; Seki, S.; Yamamoto, Y. Spherical assemblies from π -conjugated alternating copolymers: toward optoelectronic colloidal crystals. *J. Am. Chem. Soc.* **2013**, *135*, 870–876.
- Patra, A.; Chandaluri, C. G.; Radhakrishnan, T. P. Optical materials based on molecular nanoparticles. *Nanoscale* **2012**, *4*, 343–359.
- Wang, F.; Han, M. Y.; Mya, K. Y.; Wang, Y. B.; Lai, Y. H. Aggregation-driven growth of size-tunable organic nanoparticles using electronically altered conjugated polymers. *J. Am. Chem. Soc.* **2005**, *127*, 10350–10355.
- Stevens, A. L.; Kaeser, A.; Schenning, A.; Herz, L. M. Morphology-dependent energy transfer dynamics in fluorene-based amphiphile nanoparticles. *ACS Nano* **2012**, *6*, 4777–4787.
- Rong, Y.; Wu, C. F.; Yu, J. B.; Zhang, X. J.; Ye, F. M.; Zeigler, M.; Gallina, M. E.; Wu, I. C.; Zhang, Y.; Chan, Y. H.; et al. Multicolor fluorescent semiconducting polymer dots with narrow emissions and high brightness. *ACS Nano* **2013**, *7*, 376–384.
- Venkatramiah, N.; Kumar, S.; Patil, S. Femtogram detection of explosive nitroaromatics: Fluoranthene-based fluorescent chemosensors. *Chem.—Eur. J.* **2012**, *18*, 14745–14751.
- Xu, J. K.; Hou, J.; Zhang, S. S.; Xiao, Q.; Zhang, R.; Pu, S. Z.; Wei, Q. L. Electrochemical polymerization of fluoranthene and characterization of its polymers. *J. Phys. Chem. B* **2006**, *110*, 2643–2648.
- Bark, K. M.; Force, R. K. Fluorescence properties of fluoranthene as a function of temperature and environment. *Spectrochim. Acta, Part A* **1993**, *49*, 1605–1611.
- Lee, Y. H.; Wu, T. C.; Liaw, C. W.; Wen, T. C.; Guo, T. F.; Wu, Y. T. Benzo k fluoranthene-based linear acenes for efficient deep blue organic light-emitting devices. *J. Mater. Chem.* **2012**, *22*, 11032–11038.
- Chiechi, R. C.; Tseng, R. J.; Marchionni, F.; Yang, Y.; Wudl, F. Efficient blue-light-emitting electroluminescent devices with a robust fluorophore: 7,8,10-triphenylfluoranthene. *Adv. Mater.* **2006**, *18*, 325–328.
- Zhou, Y.; Ding, L.; Shi, K.; Dai, Y. Z.; Ai, N.; Wang, J.; Pei, J. A non-fullerene small molecule as efficient electron acceptor in organic bulk heterojunction solar cells. *Adv. Mater.* **2012**, *24*, 957–961.
- Nguyen, T. Q.; Doan, V.; Schwartz, B. J. Conjugated polymer aggregates in solution: Control of interchain interactions. *J. Chem. Phys.* **1999**, *110*, 4068–4078.
- Ranger, M.; Rondeau, D.; Leclerc, M. New well-defined poly(2,7-fluorene) derivatives: Photoluminescence and base doping. *Macromolecules* **1997**, *30*, 7686–7691.
- Bliznyuk, V. N.; Carter, S. A.; Scott, J. C.; Klarner, G.; Miller, R. D.; Miller, D. C. Electrical and photoinduced degradation of polyfluorene based films and light-emitting devices. *Macromolecules* **1999**, *32*, 361–369.
- Pecher, J.; Mecking, S. Nanoparticles of conjugated polymers. *Chem. Rev.* **2010**, *110*, 6260–6279.
- Teetsov, J.; Fox, M. A. Photophysical characterization of dilute solutions and ordered thin films of alkyl-substituted polyfluorenes. *J. Mater. Chem.* **1999**, *9*, 2117–2122.
- Padmanaban, G.; Ramakrishnan, S. Fluorescence spectroscopic studies of solvent- and temperature-induced conformational transition in segmented poly 2-methoxy-5-(2'-ethylhexyl)oxy-1,4-phenylenevinylene (MEHPPV). *J. Phys. Chem. B* **2004**, *108*, 14933–14941.
- Kaeser, A.; Fischer, I.; Abbel, R.; Besenius, P.; Dasgupta, D.; Gillisen, M. A. J.; Portale, G.; Stevens, A. L.; Herz, L. M.; Schenning, A. Side chains control dynamics and self-sorting in fluorescent organic nanoparticles. *ACS Nano* **2013**, *7*, 408–416.